Hindawi
Advances in Civil Engineering
Volume 2020, Article ID 3428395, 11 pages
https://doi.org/10.1155/2020/3428395

Research Article

Train Moving Load-Induced Vertical Superimposed Stress at Ballasted Railway Tracks

Heng Wang,[1] **Ling-Ling Zeng**,[2] **Xia Bian**,[3] **and Zhen-Shun Hong**[4]

[1]*School of Civil Engineering, Fujian University of Technology, Fuzhou 350108, China*
[2]*College of Civil Engineering and Architecture, Zhejiang University of Technology, Hanzhou 310014, China*
[3]*Key Laboratory of Ministry of Education for Geomechanics and Embankment Engineering, Hohai University, Nanjing 210098, China*
[4]*Institute of Geotechnical Engineering, School of Transportation, Southeast University, Nanjing 210096, China*

Correspondence should be addressed to Heng Wang; whdndx@163.com

Received 28 August 2019; Revised 17 November 2019; Accepted 14 January 2020; Published 21 February 2020

Academic Editor: Jian Ji

Ballasted railway track is an important factor that forms railway transportation over the world, which may face severe damage during operation due to the deterioration of the track ballast geometry. A practical method of evaluating train moving load-induced vertical superimposed stress in substructure by incorporating the effects of ballast characteristics and multilayered substructure is presented. The proposed method is validated by comparing with the field measurements compiled from the literature with the calculated value. It is found that the prediction accuracy of the proposed method is within ±10%, in comparison with field measurements. Meanwhile, it should be emphasized that the predicted value by traditional methods was 1.4–5.0 times field measurements. Also, key factors affecting the predicted accuracy are identified through parameter analysis by using the proposed and the traditional methods.

1. Introduction

Nowadays, a ballasted railway support system typically consists of the superstructure (track and tie) and substructure (ballast and subgrade). Train load sequentially is transmitted through superstructure, towards ballast and subgrade [1]. With the substantial increase in train speeds and axle load, the subgrade is often confronted with settlement problems at various degrees due to the rapid increase in superimposed stress transferred into subgrade [2]. Hence, it is essential to calculate the vertical superimposed stress in subgrade (σ_z) for determining train load-induced settlement. Traditionally, σ_z was empirically determined by the trapezoidal method or the Boussinesq method in practice [3–5].

Note that the trapezoidal method was established based on the assumption of the perfectly flexible loaded area between ballast and subgrade layers, and homogeneous substructure without considering the ballast characteristics [6, 7]. In practice, the load area cannot be considered as perfectly flexible. As a result, the trapezoidal method significantly overestimated the vertical stress in comparison with the field measurement [5, 8]. In addition, the ballast aggregates subjected to the cycle train loading, resulting in considerable ballast fouling, such as particle degradation, infiltration of fines from surface, subballast and subgrade infiltration, and weathering factors [2, 3, 9–21]. Therefore, the properties of ballast (the internal friction angle of ballast (φ_B) and maximum particle size ($D_{\max}$)) and stress distribution in substructure significantly varied with the real situations in practice [22–24]. Hence, the ballast characteristics should be taken into account for the determination of superimposed stress in the subgrade.

On the other hand, the Boussinesq method was based on the assumption of a homogeneous half-space for ballast and subgrade layers without considering the effect of multilayered structures [5, 7]. This assumption was far from the real condition of the railway substructure [25, 26]. This resulted

in oversimplifying actual railway conditions, eventually leading to significant overestimation of train load-induced settlements [5, 8].

This study aims at proposing a practical approach for estimating σ_z by incorporating the effects of granular characteristics and multilayered substructure. Simple equations were proposed for estimating σ_z using the particulate-probabilistic theory [27] and the Kandaurov solution [28]. The validity of the proposed equations was investigated by the comparison between computed results and field measurements. Finally, the effects of key factors of φ_B and $D_{\max}$ on σ_z were studied.

2. Proposed Empirical Equation

2.1. A Brief Review of Traditional Stress Distribution Equations. Figure 1 shows typical load distribution from wheel to the railway track, tie, ballast, and subgrade layers for standard gauge track in China and France with railway gauge of 1.435 m and tie spacing of 0.6 m. Note that P_d represents the design load; q_r is the maximum rail seat load; $\sigma_{\max}$ is tie-ballast contact pressure; L is length of the tie; L^* is the effective length of tie supporting q_r; B is the tie width; $2a$ is the average contact width between tie and ballast; h_B is the ballast layer thickness; h_n is the nth layer thickness; H_{n-1} is the equivalent depth; and Z_n is the distance from the top of nth layer. x, y, z represent the distance from load position. In the railway loading system, the rails transferred the wheel load to the ties, ballast layer, and subgrade sequentially. Thereby, tie-ballast contact stress ($\sigma_{\max}$) was essential for determining σ_z.

Generally, P_d represents the design wheel load incorporating the dynamic effects, which can be determined by the empirical relation between static load P_s and dynamic amplification factor φ, expressed as follows [2–5, 29]:

$$P_d = \varphi P_s. \tag{1}$$

Note that the calculation of φ can be practically related to the train speed by a power function based on kinematic theory [3]. As proposed by the Office of Research and Experiments of the International Union of Railways, the relation can be expressed as follows [2, 3, 5, 8]:

$$\varphi = 1 + k\left(\frac{V}{100}\right)^3, \tag{2}$$

where k was a constant depending on track and vehicle condition. Usually, $k = 0.03$ was used for common levelling defects and depressions [29]. Doyle [3] pointed out equation (2) was appropriate for the cases with $V < 200$ km/h and the maximum value of φ was 1.9. Due to the fact that there was no adequate theoretical basis for this equation, a trial analysis was required to implement equation (2) for the case $V < 200$ km/h. For the Qin-Shen railway and Orleans-Montauban railway, the measured stresses with a train speed of 5 km/h and 60 km/h are selected as the reference values, respectively. Figure 2 shows the amplification of measured stress with train speed up to 200 km/h. It can be seen that the cases investigated in this study are well evaluated by equation (2).

Based on the experiment data with various types of ties (tie spacing of 0.6 m), several researchers illustrated that only 32–76% of the wheel load was carried by the tie beneath the wheel and other parts of load were transmitted laterally to adjacent ties [2, 3]. For simplification in engineering practice, the design wheel load P_d on a rail seat was most commonly assumed distributed between three adjacent ties, and $q_r = 0.5P_d$ was suggested for the case with tie spacing of 0.6 m [2–5].

Accordingly, the uniform contact stress $\sigma_{\max}$ distribution between the effective area (BL^*) of the tie and ballast was determined as follows:

$$\begin{aligned}\sigma_{\max} &= \left(\frac{q_r}{BL^*}\right)F_2 = \left(\frac{0.5P_d}{BL^*}\right)F_2 = \left(\frac{0.5\phi P_s}{BL^*}\right)F_2 \\ &= \left(\frac{0.5P_s}{BL^*}\left(1 + k\left(\frac{V}{100}\right)^3\right)\right)F_2,\end{aligned} \tag{3}$$

where safety factor $F_2 = 2$ was recommended by AREA [4] with considering possible excessive contact pressures due to nonuniform tie support. Field measurements indicated that the maximum contact stress was exerted by the tie to the underlying ballast [5]. The trial analysis and the results from the literature [2, 5, 8] shown in Figure 2 indicated that equation (2) was suitable for the case of train speed under 200 km/h. Hence, equation (3) could be only used for calculating the train-induced dynamic stress within this range.

The effects of train speed, track and vehicle condition, and railway geometric on train loading transfer were incorporated into the calculation of $\sigma_{\max}$ in equation (3). Finally, the vertical stress σ_z can be calculated based on $\sigma_{\max}$ using the trapezoidal method or Boussinesq method without considering the effects of granular characteristics and multilayered substructure. However, there was a lack of accuracy using the traditional methods compared to the field measurements due to the oversimplification of real situations.

2.2. Proposed Equation. In practice, the track substructure layers are composed of a complex conglomeration of discrete particles, in arrays of shape, size, and varying orientations [3, 5]. Note that the average size of the railway ballast was approximately 40 mm, and their present state differs from continuum mechanics [30–33]. On the other hand, the original shape of angular particles gradually became rounded grains during the ballast fouling induced by continuous cyclic train loading. The ballast size ($D_{\max}$) and friction angle (φ_B) decreased with the increase in fouling content, resulting in a dramatic stress redistribution [22–24]. Hence, the random nature of the particles and the properties of ballast were important for evaluating the stress distribution induced by train loading.

Besides, the track substructure was a multilayered system. If the thickness of the top layer was large enough with respect to the radius of the loaded area, the multilayered system can be treated as a homogeneous layer [7]. However, the upper strata of the substructure are relatively thin in the field. For instance, the substructure of the Orleans-

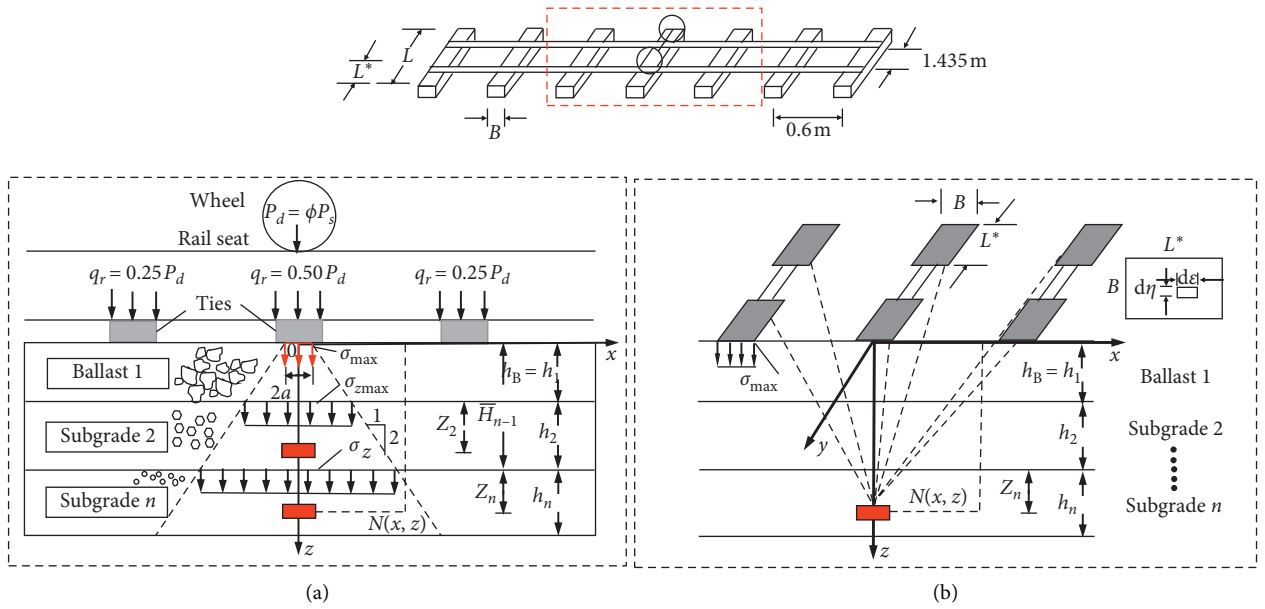

Figure 1: Schematic layout of a typical railway track system: (a) the trapezoidal method; (b) The Boussinesq method.

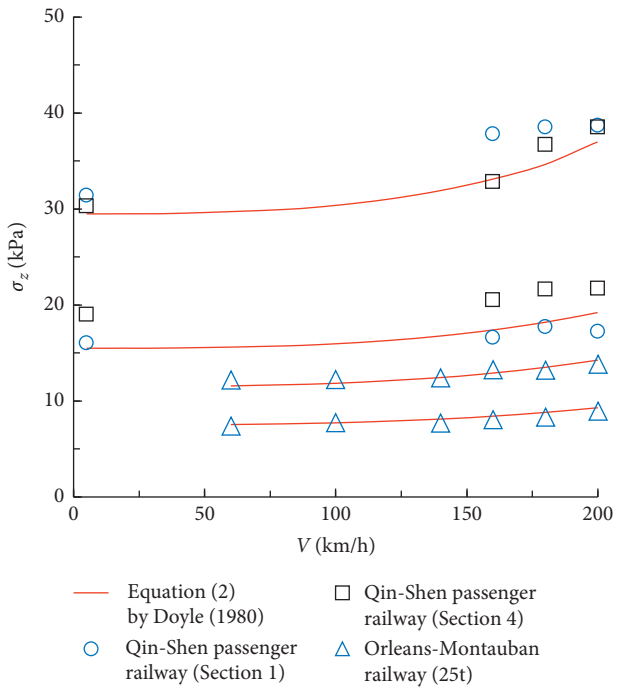

Figure 2: Measured vertical stress amplification caused by train loading.

Montauban railway in France was composed of ballast, subballast, and subgrade, with thicknesses of 0.5 m and 0.4 m for the ballast layer and subballast [8, 25, 26]. Hence, the effect of layering must be taken into consideration on train loading-induced vertical stress distribution in the railway substructure.

In summary, the following key factors need to be incorporated into the empirical equation: (1) the random nature of the discrete particles; (2) the properties of the ballast (φ_B and D_{max}); and (3) multilayered substructures. Hence, the empirical equation incorporating these factors can be proposed as follows.

2.2.1. The Random Nature of Particles. Due to the random nature of granular material, the particulate-probabilistic theory proposed by Harr [27] was adopted in this study, which was a method of estimating the distribution of expected stresses in particulate media based on the central limit theorem of probability. The calculated vertical stress acting at a point in the medium was the total accumulated effect of many random variables: the shape, size, and distribution of the particles [34]; the spatial distribution of the voids; and the transmission of vertical forces proceed from a particle to its neighbours with depth [27]. Hence, this stochastic stress diffusion method was ascendant in incorporating particulate and inherently random nature of granular material [8, 31, 35, 36]. Note that the theory described by Harr was also introduced by Wang et al. [37] for proposing a quantitative method of determining embankment load-induced vertical superimposed stress in the subsoil. Harr provided the solution of σ_z under a uniform normal load P^* acting over strip of the width $2a$ as follows:

$$\sigma_z(x,z) = P^* \times \left\{ \psi\left[\frac{x+a}{z\sqrt{\nu}}\right] - \psi\left[\frac{x-a}{z\sqrt{\nu}}\right] \right\}, \quad (4)$$

where ν is the coefficient of lateral stress and ψ is the normal cumulative Gaussian distribution function [8, 27, 37]. Under the plane-strain conditions, assume that the uniform normal load P^* equals to the tie-ballast contact stress σ_{max}, and $2a$ equals to the average contact width between tie and ballast.

2.2.2. The Friction Angle F_n. Parameter ν was the coefficient of lateral stress in equation (4), which was related to the coefficient of the lateral earth pressure at rest (K_0) and

obtained from the angle of internal friction (φ_n) of granular using Jaky's formula [38]:

$$\nu_n = K_0 = (1 - \sin\phi_n). \tag{5}$$

For the ballast layer, φ_n marked as φ_B, related to the particle shape, grain size, and stress level. It can be obtained from laboratory tests or calculated using the following empirical equation [39]:

$$\phi_B = \phi_b + \exp(d\sigma_{\max}), \tag{6}$$

where φ_b represented the true interparticle friction angle determined from the tilt table test and c and d were dimensionless coefficients. Indraratna [39] suggested the average values of $\varphi_b = 35^\circ$, $c = 31.9$, and $d = -0.002$ for the case with $\sigma_{\max} < 500$ kPa, and $C_u = 1.5$–13, $D_{\max} = 38$–80 mm, and $\phi_B = 45^\circ$–67°.

2.2.3. The Maximum Ballast Size D_{max}. Several researchers studied the distribution of tie-ballast contact stress in real track and illustrated that the typical maximum ballast size ($D_{\max}$) ranged from 48 to 70 mm and the typical width of a tie (B) ranged from 200 to 290 mm [4, 5, 39]. In other words, the typical $D_{\max}/B$ was in the range of 16.6% to 35.0%. This implies that the number of ballast particles involved indirectly supporting the tie was relatively small, which had been shown as dotted lines in Figure 3.

The contact width $2a$ was a key parameter in equation (4), and the determination of the effective support width ($2a$) was very difficult. McHenry [40] studied the effective support area between tie and ballast via laboratory tests. They estimated that the effective support area $2a/B$ varied from 21.9% to 31.2% for new ballast, and that of fouled ballast was between 28.4% and 39.7% for the case with $D_{\max} = 40$–76 mm, $C_u = 1.5$–6.5, and average axle load of 18 t. It is important to note that the values of $2a/B$ (21.9–39.7%) are approximate to the values of $D_{\max}/B$ (16.6–35.0%). Since the value of $2a/B$ and $D_{\max}/B$ was almost the same, $2a = D_{\max}$ was suggested in this study for the sake of simplicity. Therefore, the value of $2a$ represented by the typical maximum ballast size $D_{\max}$ can be obtained from the gradation of ballast material for the investigated case.

2.2.4. The Multilayered Substructures. Equation (4) can be used for determining vertical superimposed stress for a single-layer structure. However, the track substructure is a multilayered system. Based on the linear elastic theory, Odemark [41] firstly developed an empirical method to convert the multilayered system to a single-layer system, and the equivalency was calculated by the elastic moduli (E_n) and Poisson's ratio. Ullidtz [31] emphasized that this method only approximated for the case when elastic moduli decreased with depth ($E_n/E_{n+1} > 2$) and the top layer was larger compared to the radius of the load area. However, these assumptions were far from the real condition of the railway substructure. For the Orleans-Montauban railway in France, the mean moduli estimated from the penetrometer test are 133 MPa, 103 MPa, and 75 MPa for ballast, subballast, and subgrade, and the top ballast layer of 0.5 m was less than the radius of 0.52 m of the load area (BL) [8, 25, 26].

For engineering applications, Kandaurov [28] proposed a comprehensive method of multilayered equivalency by a coefficient of lateral stress ν:

$$\overline{H}_{n-1} = h_1\sqrt{\frac{\nu_1}{\nu_n}} + h_2\sqrt{\frac{\nu_2}{\nu_n}} + \sim + h_{n-1}\sqrt{\frac{\nu_{n-1}}{\nu_n}}, \tag{7}$$

where H_{n-1} represents the equivalent depth, h_n represents the layer thickness, and ν_n represents the coefficient of lateral stress of the nth layer. This method can be applied to the multilayered system for the cases of any layer thickness and variation of ν values, and no assumptions regarding stress conditions were required [7, 31]. The values of ν can be obtained from equation (5).

Combining equations (3), (5), and (7) into equation (4), the proposed equation (8) presents the general way of determining σ_z in railway multilayered substructures. The detailed derivation of the empirical solution of the proposed method is presented in the Appendix:

$$\sigma_z(x,z) = \sigma_{\max}\left[\psi\left(\frac{x + 0.5D_{\max}}{(\overline{H}_{n-1} + Z_n)(1 - \sin\phi_n)}\right) - \psi\left(\frac{x - 0.5D_{\max}}{(\overline{H}_{n-1} + Z_n)(1 - \sin\phi_n)}\right)\right]. \tag{8}$$

3. The Validity of the Proposed Method

3.1. Vertical Superimposed Stress in Substructure. A total of 63 field measurements of ten well-documented railways in China and France were used to validate the proposed method of determining σ_z [8, 42–46]. The substructure granular material properties ($D_{\max}$ and φ_n) and railway geometric parameters (P_s, V, B, L^*, h_B, and h_n) obtained from the technical specifications of the investigated cases are presented in Table 1. In the analysis, the values of φ_B are obtained by laboratory triaxial tests reported in the literature or estimated by equation (6).

The field measurements of σ_z for the ten cases discussed in this study are listed in Table 2. The different σ_z values correspond to different V or z values. For comparison, the predicted value of σ_z determined by the trapezoidal method can be calculated using the following equations [5]:

$$\sigma_z = \frac{B \cdot L^* \cdot \sigma_{\max}}{(B + z)(2L^* + z)}. \tag{9}$$

A trapezoid with 2 : 1 inclined sides was generally adopted in this method.

Besides, σ_z with the Boussinesq method can be determined by

$$\sigma_z = \sum \frac{3\sigma_{\max}}{2\pi}\int_{\varepsilon=-L^*/2}^{\varepsilon=+L^*/2}\int_{\eta=-B/2}^{\eta=+B/2} \times \frac{z^3}{\left((x-\eta)^2 + (y-\varepsilon)^2 + z^2\right)^{2.5}}\,d\varepsilon\,d\eta, \tag{10}$$

where $d\varepsilon$ and $d\eta$ are the length and width of a tie, respectively.

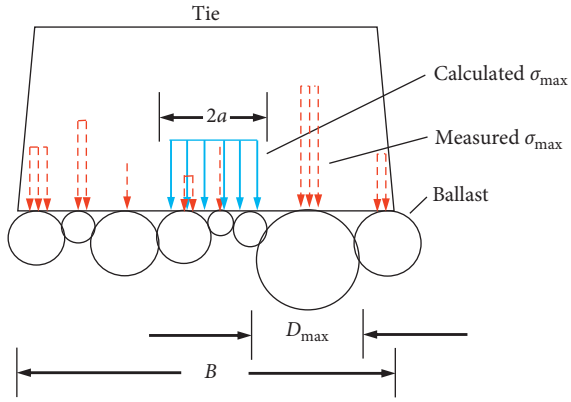

Figure 3: The average pressure distribution and actual pressure distribution at the tie-ballast interface.

Table 1: Database of railway geometric parameters in China and France.

Site	Year (y)	Axle load (t)	Track type (kg/m)	Type of ties	L^* (m)	B (m)	Ballast type	D_{max} (m)	h_B (m)	φ_B (°)	h_2 (m)	φ_2 (°)	Reference
Orleans-Montauban railway	2014	25 10.5		Concrete	1.3	0.3	Gravel	0.06	0.5	54[1]	0.4	37[1]	Lamas-lopez et al. [26] Zhang et al. [8]
Qin-Shen passenger rail line Section 1	2002	14.5	60	Concrete	1.1	0.28	Gravel	0.06	0.35	52[1]	0.4	25[1]	Nie et al. [45]
Qin-Shen passenger rail line Section 4											0.4		
Qin-Shen passenger rail line Section 2											0.6		
Da-Qin railway	2004	25	75	Concrete	1.0	0.26	Gravel	0.075	0.45	50[1]	3	30[1]	Zhao [46]
Guangzhou-Shenzhen	1994	22.5	60	Concrete	1.3	0.27	Gravel	0.048	0.45	48[2]			Li [43]
Beijing circuit railway	1993	22.5	60	Concrete	1.2	0.26	Gravel	0.06	0.35	54[2]			Li [43] Han and Zhang [42]
Xiaoshan-Ningbo	2000	22.5	60	Concrete	1.2	0.27	Gravel	0.06	0.45	49[2]			Han and Zhang [42]
Jinan-Qingdao		23		Concrete	1.1	0.29	Gravel	0.05	0.45	49[2]			Liu and Xiao [44]
Tianjin-Pukou		14		Concrete	1.3	0.29	Gravel	0.05	0.6	53[2]			Liu and Xiao [44]
Haerbin-Beian		19.6	43	Concrete	1.3	0.26	Gravel	0.06	0.4	45[2]			Li [43]
Hangzhou-Nanchang		20.1	43	Concrete	1.3	0.26	Gravel	0.06	0.4	53[2]			Li [43]
		20	43							44[2]			Li [43]

[1]Compiled from the literatures. [2]Estimated by equation (6).

Figure 4 shows the typical comparisons between the predicted value of the trapezoidal method and the measured vertical stresses. The calculated results significantly deviated from the field measurements, varying within a wide range from 1.4 to 4.0 times the measured values. Figure 5 indicates that the Boussinesq method also yields higher stresses than the field measurements, varying within a wide range from 1.9 to 5.0 times the field measurements. These behaviours indicated that the effect of granular material characteristics and multilayered substructures should be taken into account to determine σ_z.

Figure 6 shows the typical distributions of σ_z along with the depth, along with the predicted value using the proposed method (equation (8)), the trapezoidal method, and the Boussinesq method. It can be seen that the calculated results using equation (8) are in agreement with the measured ones. The comparisons between field measurements and the predicted value using different methods for the ten cases are shown in Figure 7. It is encouraged that the results predicted by the proposed method possessed a high accuracy of ±10% in comparison with the field observations. The calculated results by the trapezoidal method and Boussinesq method are also shown in the same figure. The proposed method can significantly improve the accuracy compared with the traditional methods for the cases in China and France with railway track gauge of 1.435 m, tie spacing of 0.6 m, $D_{max} = 50–80$ mm, and $\phi_B = 45°–55°$.

It should be emphasized that the standard of track spacing and tie spacing significantly varied around the world. For example, a COAL Link Line [47] with the track spacing of 1.065 m and tie spacing of 0.65 m in South Africa

Table 2: Field measurements of fourteen cases used.

Site		V (km/h)	z (m)	σ_z (kPa)	Reference
Orleans-Montauban railway		60, 100, 140, 160, 180, 200	0.96, 2.3	12.2, 12.2, 12.4, 13.2, 13.2, 13.83 7.4, 7.7, 7.7, 8.0, 8.3, 8.9	Lamas-Lopez et al. [26]
			0.96, 2.3	5.1, 5.0, 5.3, 5.4, 5.2, 5.4 1.8, 1.9, 2.1, 2.2, 2.2, 2.3	Zhang et al. [8]
Qin-Shen passenger rail line	Section 1	5, 160, 180, 200	0.35, 0.75	31.4, 37.8, 38.5, 38.7 16.0, 16.6, 17.7, 17.2	Nie et al. [45]
	Section 4		0.35, 0.75	30.3, 32.8, 36.7, 38.5 19.8, 20.5, 21.6, 21.7	
	Section 2		0.35, 0.95	32.5, 38.2, 39.4, 39.0 16.5, 18.1, 17.5, 18.2	
Da-Qin railway		75	0.45, 0.65, 0.95, 1.15, 1.45, 2.45, 3.45	32, 28, 23, 14, 10, 8, 5	Zhao [46]
Guangzhou-Shenzhen		160	0.45	35	Li [43]
Beijing circuit railway		160	0.35	120	Li [43] Han and Zhang [42]
Xiaoshan-Ningbo		120	0.45	67	Han and Zhang [42]
Jinan-Qingdao		120	0.45	33	Liu and Xiao [44]
Tianjin-Pukou		200	0.6	16	Liu and Xiao [44]
Haerbin-Beian		65	0.4	66	Li [43]
Hangzhou-Nanchang		65 70	0.4	87 68	Li [43] Li [43]

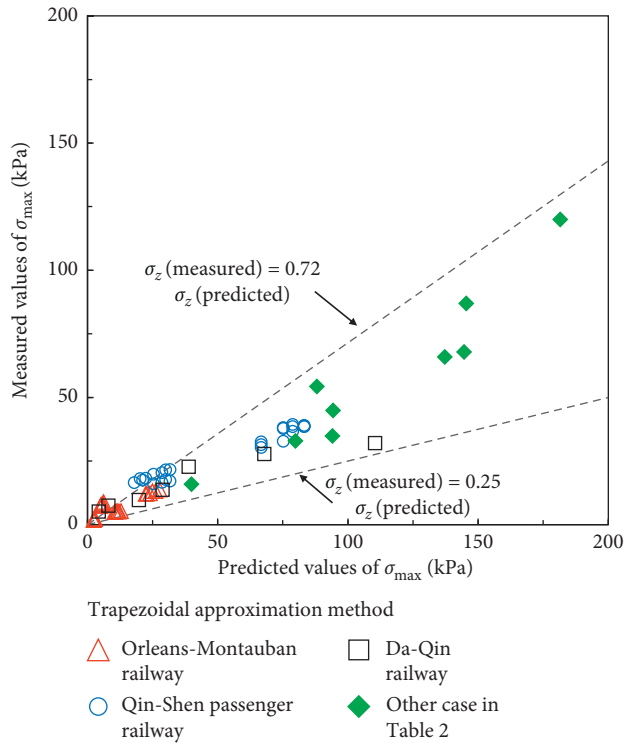

Figure 4: Comparisons between predicted results in the trapezoidal method and measured vertical stresses.

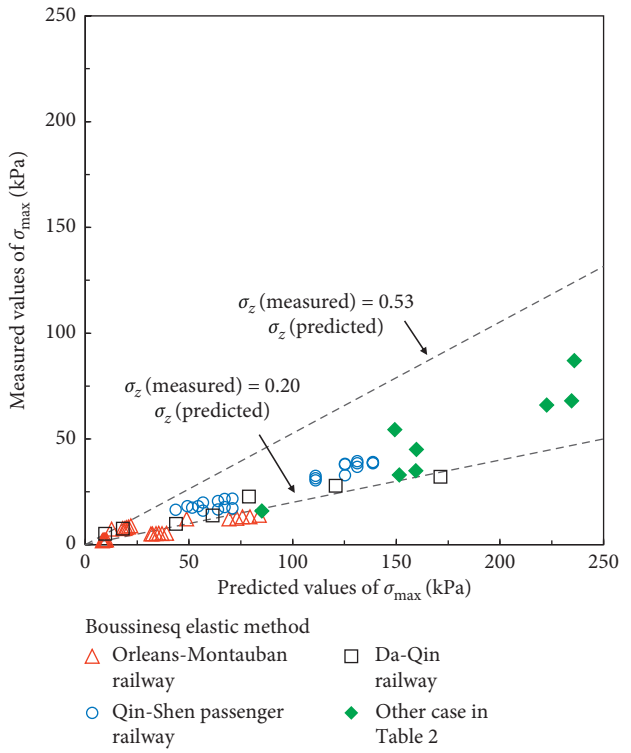

Figure 5: Comparisons between predicted results in the Boussinesq method and measured vertical stresses.

is presented in Tables 3 and 4. The maximum ballast size D_{max} was not reported in the literature and was assumed to be equal to 60 mm or 80 mm for trial analysis in this study. Figure 8 shows that the calculated results using equation (8) also have an acceptable accuracy compared with the measured ones. Due to the limited database, the application of the proposed method for cases with another standard of track spacing and tie spacing is still need to be further verified.

3.2. Parametric Analysis. With the increase in train speed and axle load in China and other countries, the ballast aggregates exhibited considerable ballast fouling due to cycle

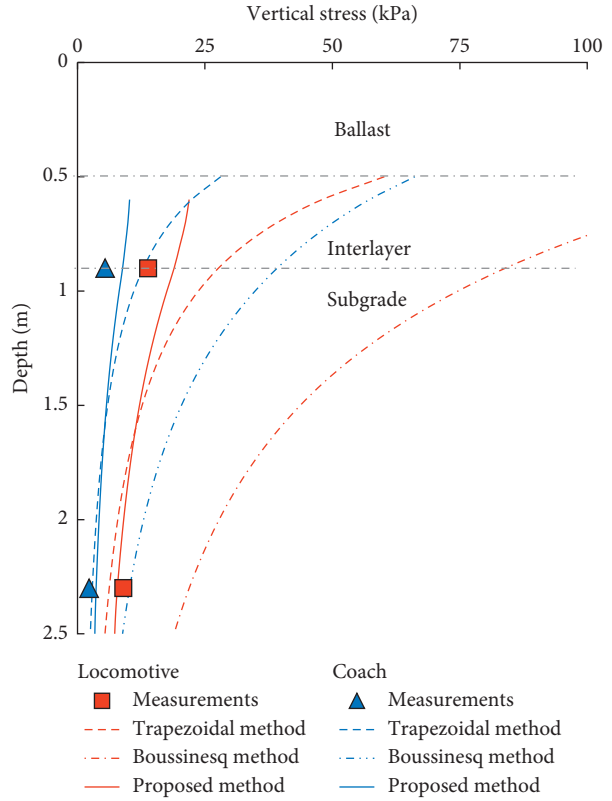

Figure 6: Stress distribution over depth calculations versus measurement at speed 200 km/h for the Orleans-Montauban railway.

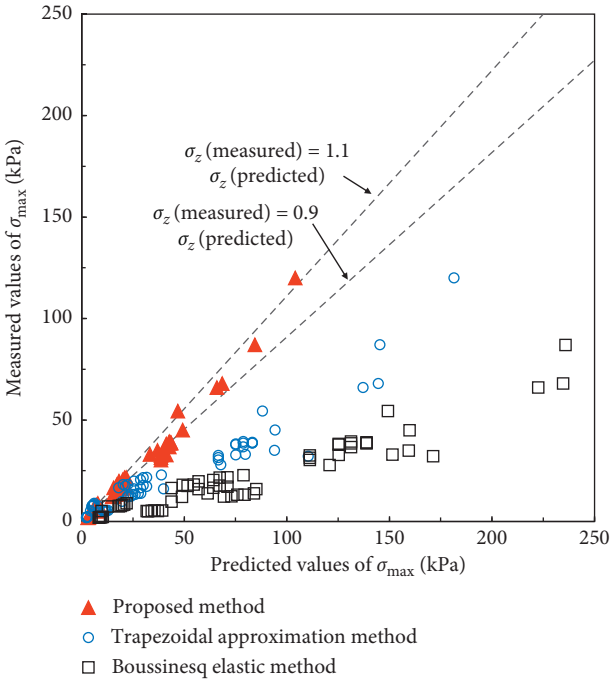

Figure 7: Comparisons between predicted results in the proposed method and measured vertical stresses.

train loading. Indraratna et al. [22] introduced the void contaminant index (VCI) for railway ballast to quantify the extent of fouling. VCI = 0% represent fresh ballast. Laboratory test results indicated that the ballast size (D_{max}) and friction angle (φ_B) decreased with the increase in VCI. When ballast was fouled, the ballast breakage of the sharp

Table 3: Database of railway geometric parameters in South Africa.

Site	Year (y)	Axle load (t)	Track type (kg/m)	Type of ties	L^* (m)	B (m)	Ballast type	D_{max} (m)	h_B (m)	φ_B (°)	h_n (m)	φ_n (°)	Reference
COAL Link Line[1]	2004	26 ∗ 2	60	Concrete	1.1	0.27	Gravel		0.3	54[2]	0.2 0.2 0.2 0.2	30[3] 25[3] 20[3] 15[3]	Yang et al. [47]

[1]Track gauge = 1.065 m; tie spacing = 0.65 m. [2]Estimated by equation (6). [3]Estimated from Figures 5 and 8 in Yang et al. [47].

Table 4: Database of railway field measurements in South Africa.

Site	V (km/h)	z (m)	σ_z (kPa)	Reference
COAL Link Line	47.5	0.5 0.7 0.9 1.1	95 85 77 60	Yang et al. [47]

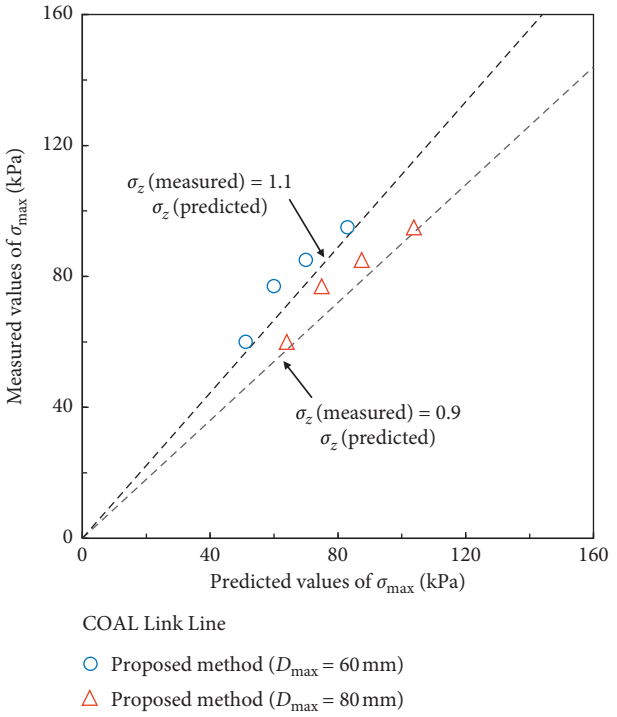

Figure 8: Comparisons between predicted results in the proposed method and measured vertical stresses for the case in South Africa.

corners and attrition of asperities occurred. The pore matrix of the ballast assembly changed substantially as the crushed fine particles clogging the voids and the number of particle contacts increased, resulting in vertical stress redistribution in the ballast layer [5]. As a result, an increasing percentage of horizontal diffuseness of train load may occur through the fine particle networks and the maximum vertical stress σ_z may reduce in the railway substructure [22–25].

To validate the application of the proposed method for simulating the above real ballast response, a parameter analysis was conducted. Section 1 of Qin-Shen passenger rail line in Table 1 was chosen for parameter analysis. Note that the calculated points located beneath the tie with a

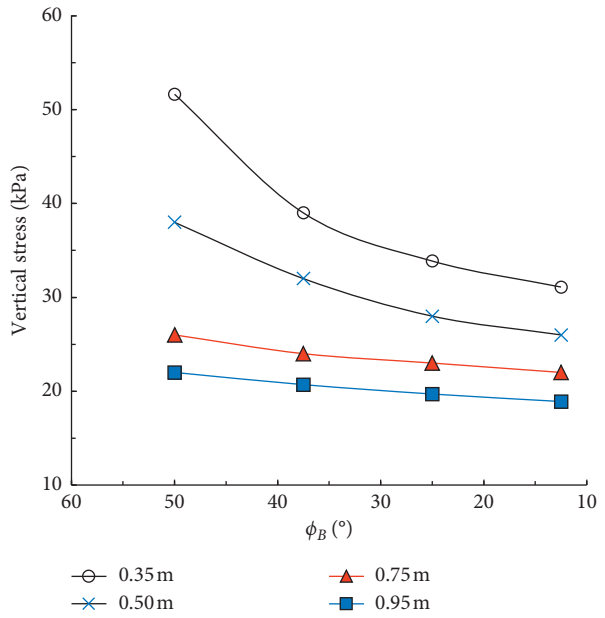

Figure 9: Maximum vertical stress in subgrade with different friction angles of ballast.

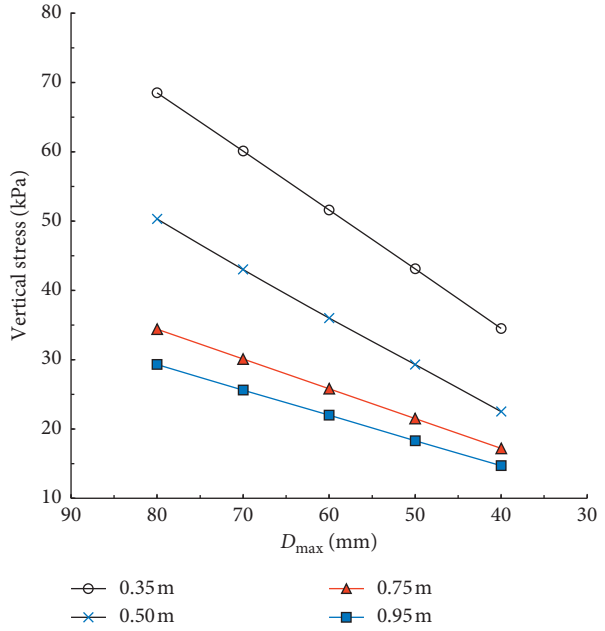

Figure 10: Maximum vertical stress in subgrade with different particle sizes.

depth of $z = 0.35$ m, 0.50 m, 0.75 m, and 0.95 m were selected for analysis. Figure 9 presents the influences of φ_B on stress distributions. $D_{\max} = 50$ mm and $\varphi_{\text{sub}} = 25^\circ$ were kept and $\varphi_B = 50^\circ$, 37.5°, 25°, 12.5° were taken into consideration. It can be seen that the maximum vertical stress σ_z decreased nonlinearly with the decrease in φ_B. In Figure 10, $\varphi_B = 50^\circ$ and $\varphi_{\text{sub}} = 25^\circ$ were kept and $D_{\max}$ varied from 80, 70, 60, and 50 to 40 mm. As expected, the maximum vertical stress σ_z decreased nonlinearly with the decreases in $D_{\max}$. These behaviours imply that the effects of ballast characteristics on train load transfer can be quantitatively evaluated using the φ_B and $D_{\max}$ by the proposed method. The decrease in maximum vertical superimposed stress for "the proposed equation with ballast characteristics" is consistent with the real ballast response under train loading.

It should be emphasized that the ballast fouling is a very complex problem, due to lack of quantitative equations describing the relationship between the extent of fouling (VCI) and $D_{\max}$ or φ_B; quantitatively assessing the fouling effect on train loading transfer is still need to be further studied. In conclusion, under the assumption that the aggregates are all connected during train loading and ignore the role of moisture on ballast fouling, the proposed method incorporating the effects of ballast characteristics (size and friction angle) and multilayered substructure on train loading transfer is recommended to empirically calculate σ_z, which only depends on the simple geometric parameters of track, the friction angle of granular material (ϕ), and the typical maximum ballast size ($D_{\max}$).

4. Conclusions

A practical method of calculating train load-induced vertical superimposed stresses in subgrade is presented by incorporating the effects of ballast characteristics and multilayered substructure on load transfer.

The proposed approach is validated based on field measurements of train load-induced vertical superimposed stresses in subgrade compiled from the literature. It is found that the calculated results with the proposed method have a good agreement with the measurements within an accuracy of ±10%, with the railway track spacing of 1.435 m, tie spacing of 0.6 m, $D_{\max} = 50$–80 mm, and $\phi_B = 45^\circ$–55°.

The proposed method incorporates the effects of ballast characteristics and multilayered substructure on vertical superimposed stresses in subgrade, substantially improving their calculating accuracy. The key influential factors responsible for ballast characteristics and multilayered substructure are found to be the maximum ballast size and the friction angle of granular material.

Notations

a: Half of the contact width between tie and ballast
B: Width of tie
c, d: Empirical coefficients
C_u: Uniformity coefficients
$D_{\max}$: Maximum particle size
F_2: Safety factor
h_B: Thickness of the ballast layer
h_n: Thickness of the nth layer
H_{n-1}: Equivalent depth
K_0: The coefficient of the lateral earth pressure at rest
k: The constant depending on track condition
L: Length of tie
L^*: Effective length of tie supporting q_r
P_d: Design load
P_s: Static load
r: The radius of a circle whose area equals to BL^*
t: Gaussian function parameters
V: Train speed
VCI: Void contaminant index
x, y, z: The distance from the load position
Z_n: The distance from the top of nth layer
q_r: Maximum rail seat load
φ: Dynamic amplification factor
φ: The internal friction angle of grain material
φ_B: The internal friction angle of ballast
φ_b: The true interparticle friction angle determined from tile table test
φ_n: The internal friction angle of nth grain layer
φ_{sub}: The internal friction angle of subgrade layer
σ_z: Vertical superimposed stress in substructure
$\sigma_{z\max}$: The maximum vertical stress applied on the subgrade
$\sigma_{\max}$: Tie-ballast contact pressure
$d\varepsilon$: The length of a tie
$d\eta$: The width of a tie
ψ: Cumulative Gaussian distribution function
ν: Coefficient of lateral stress.

Appendix

Derivation of the Proposed Equation.

The solution of σ_z under a uniform normal load P^* acting over strip of width $2a$ can be expressed as follows:

$$\sigma_z(x,z) = P^* \times \left\{ \psi\left[\frac{x+a}{z\sqrt{\nu}}\right] - \psi\left[\frac{x-a}{z\sqrt{\nu}}\right] \right\}. \tag{A.1}$$

The coefficient of lateral stress ν was taken as the coefficient of the lateral earth pressure at rest (K_0) and obtained from the angle of internal friction (ϕ_n) of granular using Jaky's formula:

$$\nu_n = K_0 = (1 - \sin\phi_n). \tag{A.2}$$

Note that $\psi(x^*)$ was the normal cumulative Gaussian distribution function expressed as follows:

$$\psi(x^*) = \int_0^{x^*} \frac{1}{\sqrt{2\pi}} e^{-(t^2/2)} dt. \tag{A.3}$$

Assuming that the uniform normal load P^* equals to the tie-ballast contact stress $\sigma_{\max}$, and $2a$ equals to the average contact width between tie and ballast, then

$$\sigma_z(x,z) = \sigma_{\max} \times \left\{ \psi\left[\frac{x+a}{z\sqrt{1-\sin\phi_n}}\right] - \psi\left[\frac{x-a}{z\sqrt{1-\sin\phi_n}}\right] \right\}. \tag{A.4}$$

The effective support width equal to the ballast maximum size was suggested in this study as follows:

$$2a = D_{\max}. \tag{A.5}$$

Hence, the σ_z at certain point $N(x,z)$ for single-layer structure can be calculated as follows:

$$\sigma_z(x,z) = \sigma_{\max} \left\{ \psi\left[\frac{x+0.5D_{\max}}{z\sqrt{1-\sin\phi_n}}\right] - \psi\left[\frac{x-0.5D_{\max}}{z\sqrt{1-\sin\phi_n}}\right] \right\}. \tag{A.6}$$

The Kandaurov method was introduced for determining the vertical stress in railway multilayered substructure:

$$\overline{H}_{n-1} = h_1\sqrt{\frac{\nu_1}{\nu_n}} + h_2\sqrt{\frac{\nu_2}{\nu_n}} + \cdots + h_{n-1}\sqrt{\frac{\nu_{n-1}}{\nu_n}}. \tag{A.7}$$

Note that the equivalent distance from the calculated point to the tie (z) can be rewritten as follows:

$$z = \overline{H}_{n-1} + Z_n. \tag{A.8}$$

Substituting equations (A.7) and (A.8) into equation (A.6) gives

$$\sigma_z(x,z) = \sigma_{\max}\left[\psi\left(\frac{x+0.5D_{\max}}{(\overline{H}_{n-1}+Z_n)(1-\sin\phi_n)} \right) - \psi\left(\frac{x-0.5D_{\max}}{(\overline{H}_{n-1}+Z_n)(1-\sin\phi_n)} \right) \right]. \tag{A.9}$$

Data Availability

The data used to support the findings of this study are included within the article.

Conflicts of Interest

The authors declare that they have no conflicts of interest.

Acknowledgments

This study was supported by the National Natural Science Foundation of China (Grant nos. 51678157 and 41977243) and Fok Ying Tung Education Foundation (Grant no. 161070).

References

[1] D. Li and E. T. Selig, "Cumulative plastic deformation for fine-grained subgrade soils," *Journal of Geotechnical Engineering*, vol. 122, no. 12, pp. 1006–1013, 1996.

[2] E. T. Selig and J. M. Waters, *Track Geotechnology and Substructure Management*, Thomas Telford, London, UK, 1994.

[3] N. F. Doyle, *Railway Track Design: A Review of Current Practice*, Australian Government Publishing Service, Canberra, Australia, 1980.

[4] American Railway Engineering Association, *Manual for Railway Engineering*, Vol. 1, American Railway Engineering Association, Lanham, MD, USA, 2013.

[5] B. Indraratna, W. Salim, and C. Rujikiatkamjorn, *Advanced Rail Geotechnology: Ballasted Track*, CRC Press, Boca Raton, FL, USA, 2011.

[6] H. J. Burd and S. Frydman, "Bearing capacity of plane-strain footings on layered soils," *Canadian Geotechnical Journal*, vol. 34, no. 2, pp. 241–253, 1997.

[7] H. Y. Fang, *Foundation Engineering Handbook*, Springer Science & Business Media, Berlin, Germany, 2013.

[8] T. W. Zhang, Y. J. Cui, F. Lamas-Lopez, N. Calon, and S. Costa D'Aguiar, "Modelling stress distribution in substructure of French conventional railway tracks," *Construction and Building Materials*, vol. 116, pp. 326–334, 2016.

[9] X. S. Shi and I. Herle, "Numerical simulation of lumpy soils using a hypoplastic model," *Acta Geotechnica*, vol. 12, no. 2, pp. 349–363, 2017.

[10] X. S. Shi, I. Herle, and D. Muir Wood, "A consolidation model for lumpy composite soils in open-pit mining," *Géotechnique*, vol. 68, no. 3, pp. 189–204, 2018.

[11] F. Zhang, Y. F. Gao, Y. X. Wu, and N. Zhang, "Upper-bound solutions for face stability of circular tunnels in undrained clays," *Géotechnique*, vol. 68, no. 1, pp. 76–85, 2018.

[12] X. Bian, Y.-J. Cui, and X.-Z. Li, "Voids effect on the swelling behaviour of compacted bentonite," *Géotechnique*, vol. 69, no. 7, pp. 593–605, 2019.

[13] X. Bian, Y.-J. Cui, L.-L. Zeng, and X.-Z. Li, "Swelling behavior of compacted bentonite with the presence of rock fracture," *Engineering Geology*, vol. 254, pp. 25–33, 2019.

[14] L. L. Zeng, Y. Q. Cai, Y. J. Cui, and Z. S. Hong, "Hydraulic conductivity of reconstituted clays based on intrinsic compression," *Géotechnique*, vol. 70, no. 3, pp. 268–275, 2020.

[15] W. J. Cen, J. R. Luo, W. D. Zhang, and M. S. Rahman, "An enhanced generalized plasticity model for coarse granular material considering particle breakage," *Advances in Civil Engineering*, vol. 2018, Article ID 7242936, 9 pages, 2018.

[16] J. Li, J. L. Zheng, Y. S. Yao, J. H. Zhang, and J. H. Peng, "Numerical method of flexible pavement considering moisture and stress sensitivity of subgrade soils," *Advances in Civil Engineering*, vol. 2019, Article ID 7091210, 10 pages, 2019.

[17] J. W. Yang, J. M. Zhao, and X. S. Liu, "Numerical study on the evolution of agglomerate breakage and microstructure of angular gravel in cyclic soil-structure interface test," *Advances in Civil Engineering*, vol. 2019, Article ID 7232613, 24 pages, 2019.

[18] J. R. Zhang and B. Zhang, "Fractal pattern of particle crushing of granular geomaterials during one-dimensional compression," *Advances in Civil Engineering*, vol. 2018, Article ID 2153971, 14 pages, 2018.

[19] D. L. He and Y. H. Cheng, "Numerical simulation for mechanical behavior of asphalt pavement with graded aggregate base," *Advances in Civil Engineering*, vol. 2018, Article ID 1404731, 9 pages, 2018.

[20] X. Bian, Y.-J. Cui, L.-L. Zeng, and X.-Z. Li, "State of compacted bentonite inside a fractured granite cylinder after infiltration," *Applied Clay Science*, vol. 186, Article ID 105438, 2020.

[21] X. S. Shi, J. Y. Nie, J. D. Zhao, and Y. F. Gao, "A homogenization equation for the small strain stiffness of gap-graded granular materials," *Computers and Geotechnics*, vol. 121, Article ID 103440, 2020.

[22] B. Indraratna, L.-j. Su, and C. Rujikiatkamjorn, "A new parameter for classification and evaluation of railway ballast

fouling," *Canadian Geotechnical Journal*, vol. 48, no. 2, pp. 322–326, 2011.

[23] B. Indraratna, N. T. Ngo, C. Rujikiatkamjorn, and J. S. Vinod, "Behavior of fresh and fouled railway ballast subjected to direct shear testing: discrete element simulation," *International Journal of Geomechanics*, vol. 14, no. 1, pp. 34–44, 2014.

[24] B. Indraratna, N. Tennakoon, S. Nimbalkar, and C. Rujikiatkamjorn, "Behaviour of clay-fouled ballast under drained triaxial testing," *Géotechnique*, vol. 63, no. 5, pp. 410–419, 2013.

[25] Y.-J. Cui, F. Lamas-Lopez, V. N. Trinh et al., "Investigation of interlayer soil behaviour by field monitoring," *Transportation Geotechnics*, vol. 1, no. 3, pp. 91–105, 2014.

[26] F. Lamas-Lopez, Y.-J. Cui, N. Calon, S. Costa D'Aguiar, M. Peixoto De Oliveira, and T. Zhang, "Track-bed mechanical behaviour under the impact of train at different speeds," *Soils and Foundations*, vol. 56, no. 4, pp. 627–639, 2016.

[27] M. E. Harr, *Mechanics of Particulate media: A Probabilistic Approach*, AmericanMcGrawHill, New York, NY, USA, 1977.

[28] I. I. Kandaurov, *Mechanics Of Discrete Media and Its Application to Construction*, Izd. Liter Po Stroitel'stvu, Russia, 1966, in Russian.

[29] X. Bian, H. Jiang, C. Cheng, Y. Chen, R. Chen, and J. Jiang, "Full-scale model testing on a ballastless high-speed railway under simulated train moving loads," *Soil Dynamics and Earthquake Engineering*, vol. 66, pp. 368–384, 2014.

[30] D. Heath, J. Waters, M. Shenton, and R. Sparrow, "Design of conventional rail track foundations," *Proceedings of the Institution of Civil Engineers*, vol. 51, no. 2, pp. 251–267, 1972.

[31] P. Ullidtz, *Modelling Flexible Pavement Response and Performance*, Narayana Press, Odder, Denmark, 1998.

[32] W. L. Lim and G. R. McDowell, "Discrete element modelling of railway ballast," *Granular Matter*, vol. 7, no. 1, pp. 19–29, 2005.

[33] M. Lu and G. McDowell, "The importance of modelling ballast particle shape in the discrete element method," *Granular Matter*, vol. 9, no. 1-2, pp. 69–80, 2006.

[34] X. S. Shi, J. Zhao, J. Yin, and Z. Yu, "An elastoplastic model for gap-graded soils based on homogenization theory," *International Journal of Solids and Structures*, vol. 163, pp. 1–14, 2019.

[35] P. L. Bourdeau and M. E. Harr, "Stochastic theory of settlement of loose cohesionless soils," *Géotechnique*, vol. 39, no. 4, pp. 641–654, 1989.

[36] J. H. Schmertmann, "Stress diffusion experiment in sand," *Journal of Geotechnical and Geoenvironmental Engineering*, vol. 131, no. 1, pp. 1–10, 2005.

[37] H. Wang, L. L. Zeng, X. Bian, and Z. S. Hong, "Evaluation of vertical superimposed stress in subsoil induced by embankment loads," *International Journal of Geomechanics*, vol. 19, no. 1, 2019.

[38] J. Jaky, "The coefficient of earth pressure at rest," *Journal for Society of Hungarian Architects and Engineers*, vol. 78, no. 22, pp. 355–358, 1944.

[39] B. Indraratna, D. Ionescu, and H. D. Christie, "Shear behavior of railway ballast based on large-scale triaxial tests," *Journal of Geotechnical and Geoenvironmental Engineering*, vol. 124, no. 5, pp. 439–449, 1998.

[40] M. T. McHenry, "*Pressure measurement at the ballast-tie interface of railroad track using matrix based tactile surface sensors*," M.S. thesis, University of Kentucky, Lexington, KY, USA, 2013.

[41] N. Odemark, *Undersokning av Elasticitetegenskaperna hos Olika Jordarter samt Teori for Berakning av Belagningar Eligt Elasticitesteorin*, Statens Vaginstitute, Linköping, Sweden, 1949.

[42] Z. L. Han and Q. L. Zhang, "Dynamic stress analysis on speed increase subgrade of existing railway," *China Railway Science*, vol. 26, no. 5, pp. 1–5, 2005.

[43] Z. C. Li, *Study on the vertical load transmission through the track structure and the characteristics of subgrade dynamic stresses*, Ph.D. thesis, China Academy of Railway Sciences, Beijing, China, 2000.

[44] J. Liu and J. Xiao, "Experimental study on the stability of railroad silt subgrade with increasing train speed," *Journal of Geotechnical and Geoenvironmental Engineering*, vol. 136, no. 6, pp. 833–841, 2010.

[45] Z. H. Nie, B. Ruan, and L. Li, "Testing and analysis on dynamic performance of subgrade of Qinshen railway," *Journal of Vibration and Shock*, vol. 24, no. 2, pp. 30–32, 2005.

[46] X. Zhao, "*Study on the assessment theory and measures of subgrade quality of Datong-Qinhuangdao heavy load railway*," M.S. thesis, Beijing Jiaotong University, Beijing, China, 2011.

[47] L. A. Yang, W. Powrie, and J. A. Priest, "Dynamic stress analysis of a ballasted railway track bed during train passage," *Journal of Geotechnical and Geoenvironmental Engineering*, vol. 135, no. 5, pp. 680–689, 2009.